

Communication

Evidence of the spin Seebeck effect in Ni-Zn ferrites polycrystalline slabs



J.D. Arboleda^{a,*}, O. Arnache^a, M.H. Aguirre^{b,c,d,e}, R. Ramos^f, A. Anadón^g,
M.R. Ibarra^{b,c,d,e}

^a Instituto de Física, Universidad de Antioquia, A.A. 1226, Medellín, Colombia

^b Instituto de Nanociencia de Aragón, Universidad de Zaragoza, E-50018 Zaragoza, Spain

^c Laboratorio de microscopías avanzadas, Universidad de Zaragoza, Zaragoza, Spain

^d Fundación INA, E-50018 Zaragoza, Spain

^e Departamento de Física de la Materia Condensada, Universidad de Zaragoza, E-50009 Zaragoza, Spain

^f Advanced Institute for Materials Research, Tohoku University, Sendai 980-8577, Japan

^g IMDEA Nanociencia, Campus de Cantoblanco, 28049 Madrid, Spain

ARTICLE INFO

Keywords:

Spin Seebeck effect

Spin caloritronics

Ni-Zn ferrites

ABSTRACT

We report on the observation of the spin Seebeck effect in Ni-Zn ferrites slabs with different Zn concentration. All samples have a spinel structure confirmed by XRD and TEM. We fully characterize the magnetic properties by VSM and Mössbauer spectroscopy. Samples exhibit a nonmonotonic magnetization behavior depending on the structural inversion parameter, however we found a spin Seebeck response voltage of about 25.5 nV/K independent of the magnetization and the inversion degree.

1. Introduction

The generation of spin current induced by an applied thermal gradient via the spin Seebeck effect (SSE) [1] is one of the most remarkable effects in the growing field of spin caloritronics [2,3]. The SSE has been observed in a great variety of materials with different electrical (conductors [4] and insulators [5,6]) and magnetic (ferromagnetic or ferrimagnetic, weak ferromagnetic [7], antiferromagnetic [8,9], and paramagnetic [10]) properties, both in thin film, including heterostructures [11,12], and bulk materials [5,13–16].

The SSE is a thermoelectric effect mediated by the spin degree of freedom. When a magnetic material (FM) is subjected to a temperature gradient generates a spin current parallel to the thermal gradient. This spin current is detected in an attached normal metal (NM), with high spin-orbit coupling, as an electromotive force by means of the inverse spin Hall effect (ISHE) [17].

Despite the intense work being carried out by different research groups, the mechanism underlying the SSE is still under discussion [18–22]. The role of the magnetic order, the different length scales of the materials involved, effects at the interface, the surface magnetization, among others, are still active research lines [23–25], e. g. in YIG, Aqeel et al. [26] demonstrated that surface properties strongly influence the SSE response by preparing samples with different surface quality.

On the other hand, Kalappattil et al. [27], very recently, reported surface magnetic anisotropy dependence in bulk YIG slabs, showing the importance of surface magnetization in the SSE measurements.

We recently reported the observation of SSE in the weak ferromagnetic Zn ferrite [7] with considerable voltage response despite the negligible magnetization. This result suggests that the SSE signal is independent of the FM magnetization saturation. The SSE in these types of ferrites might be also influenced by the surface magnetization in the FM.

The SSE in the longitudinal configuration has been investigated in a variety of spinel ferrites such as Cobalt [28,29], Nickel [30,31] and Zinc ferrites [7], especially in thin films. In this paper we systematically investigated the saturation magnetization dependence of the SSE in the isostructural spinel Ni-Zn ferrites by varying the Ni and Zn content.

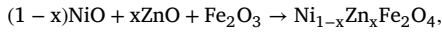
2. Experimental procedure

Samples consist of a series of polycrystalline Ni-Zn ferrites (NZFO) slabs with a mechanically polished surface on which 8.5 ± 0.5 nm Pt film was sputtered for ISHE detection. The well polished surface allows flat deposition free from defects at the interface, even through different grains as shown in Fig. 1(a). All samples were prepared using the standard solid state reaction method, mixing thoroughly the oxides

* Corresponding author.

E-mail address: juan.arboledaj@udea.edu.co (J.D. Arboleda).

with the proper stoichiometric amounts according to equation:



with $x = 0, 0.3, 0.4, 0.5, 0.7$ and 1 . The corresponding notation in what follows will be NFO, NZFO_30, NZFO_40, NZFO_50, NZFO_70 and ZFO, where NFO and ZFO correspond to Ni and Zn ferrite respectively, and the number indicates the Zn percentage of each sample relative to Ni content. The raw materials were powders of ZnO (Merk 99%), NiO (99.9%) and $\alpha\text{-Fe}_2\text{O}_3$ (Merk 99.9%). Resulting mixture were calcined in air at 1150°C for 12 h, then were pressed uniaxially into rectangular shaped slabs with dimensions of $7.0 \times 2.0 \times 0.5 \text{ mm}^3$ as shown in Fig. 1(b), and finally were sintered at 1300°C for 24 h. We performed structural and magnetic characterization by using X-ray diffraction (XRD), Scanning/Transmission electron microscope with high Angular Annular dark field (STEM-HAADF) detector, vibrating sample magnetometry (VSM) and Mössbauer spectroscopy methods.

We performed the SSE measurements in the longitudinal configuration where a spin current is induced from the NZFO slab to the Pt layer due to a temperature difference (ΔT) applied across the NZFO/Pt bilayer structure (z-direction) in the presence of a magnetic field par-

allel to the interface (x-direction). The spin current is converted into an electric voltage (y-direction) by means of the ISHE in the Pt layer. Nowadays it is known that effects of temperature difference in the thermal contacts can affect the magnitude of the SSE signal, as was recently demonstrated by Sola et al. [32]. We also measured the anomalous Nernst effect (ANE) [33] in the FM, and the proximity anomalous Nernst effect (PANE) in the deposited NM in order to rule out spurious signals. ANE was the same geometric configuration as the SSE. The absence of the proximity induced anomalous Nernst effect was also confirmed by measurements under an in-plane thermal gradient and a magnetic field applied perpendicular to the NZFO/Pt interface [34]. More details are available in the previous study mentioned above in Ref. [7].

3. Results and discussion

The XRD patterns indicate the formation of a single phase of pure spinel structures [Fig. 1(c)] with the configuration $[\text{Zn}_x\text{Fe}_{1-x}]_A[\text{Ni}_{1-x}\text{Fe}_{1+x}]_B\text{O}_4$, where A and B denote tetrahedral and octahedral sites respectively, in the AB_2O_4 spinel structure [35]. The parameter $\delta = 1 - x$ determined the degree of inversion of the structure, thus for $\delta = 0$ ($x = 1$) we have normal spinel structure (ZFO); for $\delta = 1$ ($x = 0$) inverse spinel (NFO); and for intermediate values ($0 \leq \delta \leq 1$) mixed spinel (NZFO). The magnetic properties are directly dependent on this parameter δ as shown below. In particular a small δ value, less than 0.04, is responsible for a weak ferromagnetic behavior in our samples of ZFO (see Ref. [7]).

The diffraction peaks shift towards lower 2θ values as a function of Zn content, indicating an increase of lattice parameter. The refined values of lattice parameter [Fig. 1(d)] display a linear dependence with Zn concentration. We can explain this behavior by adding the different ionic radii [36] ($[\text{Zn}^{2+}]_A = 0.600 \text{ \AA}$; $[\text{Fe}^{3+}]_A = 0.490 \text{ \AA}$; $[\text{Ni}^{2+}]_B = 0.690 \text{ \AA}$; $[\text{Fe}^{3+}]_B = 0.645 \text{ \AA}$) for a unit formula of NZFO as follows:

$$\begin{aligned} x[\text{Zn}^{2+}]_A + (1-x)[\text{Fe}^{3+}]_A + (1-x)[\text{Ni}^{2+}]_B + (1+x)[\text{Fe}^{3+}]_B \\ = 1.825 + 0.065x, \end{aligned}$$

which indicates that the total ionic radius linearly increases when Zn is incorporated into the structure. The same dependence has been previously reported [37–40], but with a slightly different interpretation.

We study the crystal structure of all the samples by mean of STEM-HAADF. Fig. 2(a) shows a general profile of lamella $\text{Ni}_{0.6}\text{Zn}_{0.4}\text{Fe}_2\text{O}_4$. Coherent grains with a size of several microns can be clearly distinguished. The Pt layer is composed by nanograins in the range of 5–10 nm [see Fig. 1(a)]. High resolution STEM-HAADF image of a grain boundary [Fig. 2(b)] shows two typical grain orientations in perfect agreement with spinel structure, as confirmed by the diffraction pattern in Fig. 2(c).

Atomic percentages obtained by SEM-EDX are in accordance with the nominal composition as shown in Table 1. An EDS analysis using TEM was performed on a $1 \mu\text{m}$ line through a grain boundary in all samples. The elemental composition is homogeneous despite passing through two different grains. It can be ensured that there are no significant structural defects in grain boundaries.

The magnetization results [Fig. 3(a)] show that all NZFO slabs present a soft magnetic behavior with low coercive fields for all compositions. A non-monotonic variation of saturation magnetization depending on the inversion parameter δ is presented in Fig. 3(b). Magnetic measurements were made before and after Pt deposition. As can be seen in Fig. 3(c), the NZFO slabs show a magnetic anisotropy with in plane easy axis. Additionally, we ensure that Pt film deposited on the top surface does not significantly affect the bulk magnetic properties of the sample. Magnetism in spinel ferrites is well explained on reference [35]. In a complete normal spinel structure ($\delta = 1$), ZFO presents paramagnetic behavior at room temperature and have a Neel

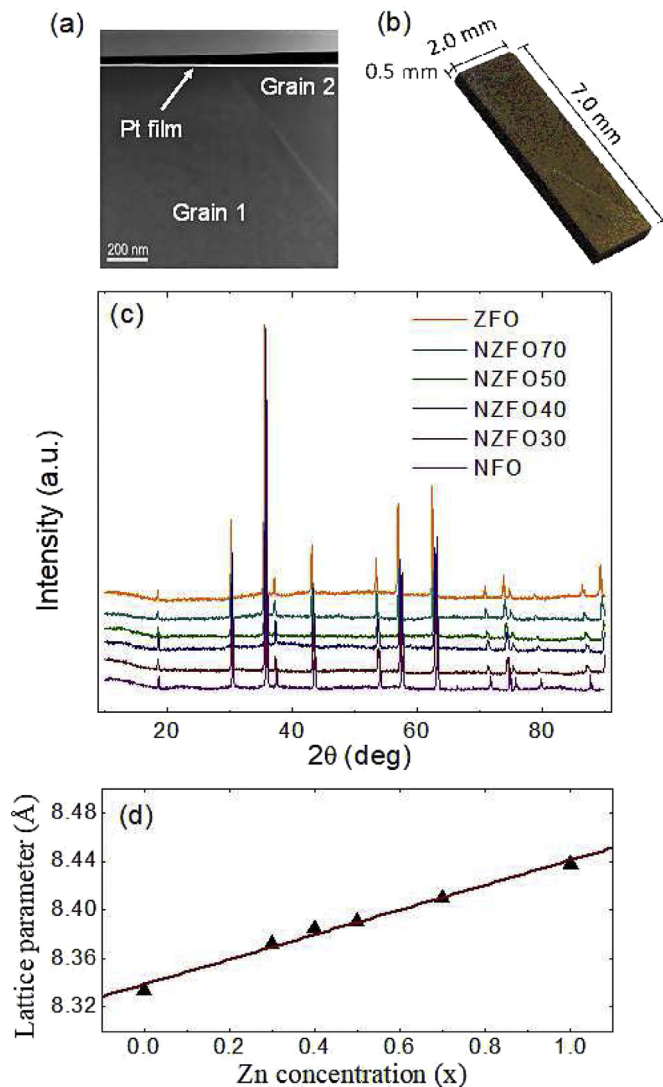


Fig. 1. (a) Detail of Platinum deposition. Thickness of Pt layer $\approx 8.5 \text{ nm}$. (b) Photograph of a uniaxially pressed and sintered sample after polishing. (c) XRD patterns of Ni-Zn ferrites. Zn content increases from bottom to top. (d) Zn concentration dependence of lattice parameter.

Download English Version:

<https://daneshyari.com/en/article/7988024>

Download Persian Version:

<https://daneshyari.com/article/7988024>

[Daneshyari.com](https://daneshyari.com)